Electronic Supplementary Material (ESI) for Journal of Materials Chemistry C

Supporting Information

Highly Luminescent Chameleon: Fine-Tuned Emission Trajectory and Controllable Energy Transfer

Huabin Zhang,[a,b] Xiaochen Shan,[a,b] Zuju Ma,[a,b] Liujiang Zhou,[a,b] Mingjian Zhang,[a,b] Ping Lin,[a] Shengmin Hu,[a] En Ma,[a] Renfu Li,[a] and Shaowu Du*[a]

[a] *State Key Laboratory of Structural Chemistry, Fujian Institute of Research on the Structure of Matter, Chinese Academy of Sciences, Fuzhou, Fujian 350002, P. R. China.* [b] *Graduate University of Chinese Academy of Sciences, Beijing 100039, P. R. China.*

*Corresponding author, E-mail: swdu@fjirsm.ac.cn. Fax: 86-591-83709470.

1. Experimental procedures

1.1 Materials and Instruments.

All the chemicals were purchased commercially and used as received. Thermogravimetric experiments and mass spectra were performed using Thermal Analysis-Quadrupole Mass Spectrometer TGA/NETZSCH STA449C instrument heated from 30–1000 ºC (heating rate of 10 ºC /min, nitrogen stream). The powder X-ray diffraction (XRD) patterns were recorded on crushed single crystals in the 2θ range 5–50º using Cu-Kα radiation. The XRD were measured on a PANalytical X'pert PRO X-Ray Diffractometer. IR spectra using the KBr pellet technique were recorded on a Spectrum-One FT-IR spectrophotometer. Elemental analyses were measured with an Elemental Vairo EL III Analyzer. Inductively coupled plasma spectroscopy (ICP) was performed on a Thermo IRIS Intrepid II XSP spectrometer. Fluorescence spectra for the solid samples were performed on an Edinburgh Analytical instrument FLS920. Quantitative data were measured in the solid state at 298±2 K with excitation and emission slit widths of 2/1.3 nm, and the emission was monitored from 400 to 750 nm. The overall luminescent quantum yields of the solid-state samples were determined by an absolute method using an integrating sphere (150 mm diameter, $BaSO_4$ coating) on Edinburgh Instrument FLS920 and acquired by the following formula:

$$\Phi_{\text{overall}} = \frac{A_H}{R_{ST} - R_H}$$

where A_H is the area under emission spectrum of the sample and R_{ST} and R_H are diffuse reflectance of the reflecting standard and the sample, respectively. The concrete operation for the solid-state quantum yield determination was based on a previously reported technique.[1] Reported overall luminescent quantum yields were averages of at least three independent determinations. The estimated errors for quantum yields and luminescent lifetimes are within 5%. Luminescence lifetime of compound **2** was obtained by reconvolution exponential fitting of experimental data

based on least square method. The details of this approach have been discussed elsewhere (A. Beeby, S. Faulkner, *Chem. Phys. Lett*. 1997, **266**, 116).

1.2 Synthesis

1.2.1 Synthesis for [Eu(BTB)(DMSO)$_2$]·H$_2$O (1)

In a typical reaction, a mixture of Eu(NO$_3$)$_3$·6H$_2$O (0.1133 g, 0.25 mmol) and H$_3$BTB (1,3,5-Tris(4-carboxyphenyl)benzene) (0.110 g, 0.25 mmol) were placed in a 20 mL of Teflon-lined stainless steel vessel with 6 mL of mixed-solvent of DMF and DMSO (V/V = 1:1). The mixture was heated to 120 ºC in 4 h and kept to this temperature for 3 days. The reaction system was cooled slowly to room temperature during another 2 days. Colourless prismatic crystals of **1** were collected in 53% yield based on Eu(NO$_3$)$_3$·6H$_2$O (Fig. S5). Elemental analysis calcd. for **1** C$_{31}$H$_{29}$EuO$_9$S$_2$ (761.61): C, 48.88; H, 3.84; S, 8.42%. Found: C, 49.16; H, 3.61; S, 8.34%.

1.2.2 Synthesis for [Gd(BTB)(DMSO)$_2$]·H$_2$O (2), [Tb(BTB)(DMSO)$_2$]·H$_2$O (3) and [Eu$_{0.0040}$Tb$_{0.0460}$ Gd$_{0.9500}$(BTB)(DMSO)$_2$]·H$_2$O (4).

Compounds **2** and **3** were synthesized in 38% and 42% yields, respectively by the similar method as described for **1**, except that the corresponding Gd(NO$_3$)$_3$·6H$_2$O and Tb(NO$_3$)$_3$·6H$_2$O were used instead of Eu(NO$_3$)$_3$·6H2O. Elemental analysis calcd. for **2** C$_{31}$H$_{29}$GdO$_9$S$_2$ (766.94): C 48.55, H 3.81, S 8.36%; found: C 47.96, H 3.63, S 8.59%. For **3** C$_{31}$H$_{29}$TbO$_9$S$_2$ (768.61): C 48.44, H 3.80, S 8.34%; found: C 49.16, H 4.03, S 8.67%. Similarly, the mixed-lanthanide compound **4** was synthesized by using a mixture of Eu(NO$_3$)$_3$·6H$_2$O, Tb(NO$_3$)$_3$·6H$_2$O and Gd(NO$_3$)$_3$·6H$_2$O.

1.3 X-ray Crystallography

Single-crystal X-ray diffraction data were collected on a Rigaku diffractometer with a Mercury CCD area detector (Mo Kα; λ = 0.71073Å) at room temperature. Empirical absorption corrections were applied to the data using the Crystal Clear program. The structures were solved by the direct method and refined by the full-matrix least-squares on F^2 using the SHELXTL-97 program. Metal atoms in each compound were located from the *E*-maps and other non-hydrogen atoms were located in successive difference Fourier syntheses. All non-hydrogen atoms were refined anisotropically. The organic hydrogen atoms were positioned geometrically. The

lattice molecules were severely disordered and are unsuccessfully located. Thus, they were removed using the SQUEEZE routine of PLATON. Crystallographic data and other pertinent information are summarized in Table S1.

1.4 Basic Characterization

The simulated and experimental XRD patterns of compounds **1**−**4** obtained at room temperature are shown in Fig. S1. Their peak positions correspond well with each other, indicating the phase purity of the solids. The difference in reflection intensities between the simulated and experimental patterns may be due to variation in the preferred orientation of the powder samples during collection of the experimental XRD data.[2] In the IR spectra of **1**–**4** (Fig. S2), the absence of strong absorption associated with the carboxyl group at around 1700 cm^{-1} indicates that the H_3BTB ligand is completely deprotonated, as also confirmed by the X-ray analysis. Not only the XRD patterns but also the IR spectra for compounds **1**–**4** are similar to each other, which confirm the fact that they are isomorphic.

Thermogravimetric analysis (TGA) was carried out to examine the thermal stability of **1**–**4** (Fig. S3). The samples were heated up to 1000 ºC under nitrogen gas and they exhibit similar thermal behaviour. TGA curves for **1**–**4** all exhibit two steps of weight losses, with the first weight loss occurring between around 100 and 100–350 ºC corresponding to the loss of the lattice water molecules and the coordinated DMSO molecules. No obvious weight loss is observed from 350 to 500 ºC. After that, a sharp decomposition of the frameworks start. The existence and departure of the guest water molecular and the coordinated DMSO can be detected on thermal analysis-quadrupole mass spectrometer (Fig. S4).

Reference

1. (a) Q. Zhu, C. Shen, C. Tan, T. Sheng, S. Hu and X. Wu. *Chem. Commun.*, 2012, **48**, 531–533; (b) J. C. Mello, H. F. Wittmann, and R. H. Friend. *Adv. Mater.*, 1997, **9**, 230–232.
2. (a) H. Zhang, X. Shan, L. Zhou, P. Lin, R. Li, E. Ma, X. Guo and S. Du. *J. Mater. Chem C.*, 2013, **1**, 888-891. (b) N. Jeong, B. Samanta, C. Lee, O. K. Farha, and J. T. Hupp. *J. Am. Chem. Soc.*, 2012, **134**, 51−54.

Table S1 Pertinent Crystal Data and Structure Refinement Results for **1**–**3**.

Compounds	**1**	**2**	**3**
Formula	$C_{31}H_{29}EuO_9S_2$	$C_{31}H_{29}GdO_9S_2$	$C_{31}H_{29}TbO_9S_2$
CCDC	930171	930172	930173
M (g mol^{-1})	761.61	766.94	768.61
Crystal system	Monoclinic	Monoclinic	Monoclinic
Space group	*C*2/*c*	*C*2/*c*	*C*2/*c*
a (Å)	33.232(1)	33.226(7)	33.181(8)
b (Å)	10.346(4)	10.372(2)	10.296(2)
c (Å)	27.852(1)	27.776(6)	27.814(6)
β (°)	106.872(7)	107.061(4)	107.239(2)
V (Å^3)	9164(6)	9151(3)	9075(3)
Z	8	8	8
D_c (g cm^{-3})	1.078	1.087	1.099
□*μ* (mm^{-1})	1.493	1.573	1.683
F(000)	2976	2984	2992
GOF	1.215	1.092	1.063
R_1[a]	0.0853	0.0398	0.0433
	(0.0969)[b]	(0.0466)[b]	(0.0495)[b]
wR_2[a]	0.1836	0.0851	0.0912
	(0.1893)[b]	(0.0878)[b]	(0.0939)[b]

[a] $R = \sum (||F_o| - |F_c||)/\sum |F_o|$, $wR = \{ \sum w[(F_o^2 - F_c^2)^2]/\sum w[(F_o^2)^2]\}^{1/2}$;

[b] Based on all data.

Table S2 The CIE coordinates of emissions for **4** excited at different wavelengths.

Excitation (nm)	CIE *x*	CIE *y*
315	0.41	0.41
320	0.4	0.41
325	0.4	0.4
330	0.4	0.4
335	0.41	0.4
340	0.39	0.38
341	0.39	0.38
342	0.39	0.37
343	0.39	0.36
344	0.38	0.36
345	0.38	0.35
346	0.37	0.34
347	0.36	0.33
348	0.35	0.32
349	0.34	0.3
350	0.32	0.29
351	0.31	0.27
352	0.3	0.25
353	0.27	0.22
354	0.27	0.22
355	0.25	0.2
360	0.2	0.14
365	0.19	0.13

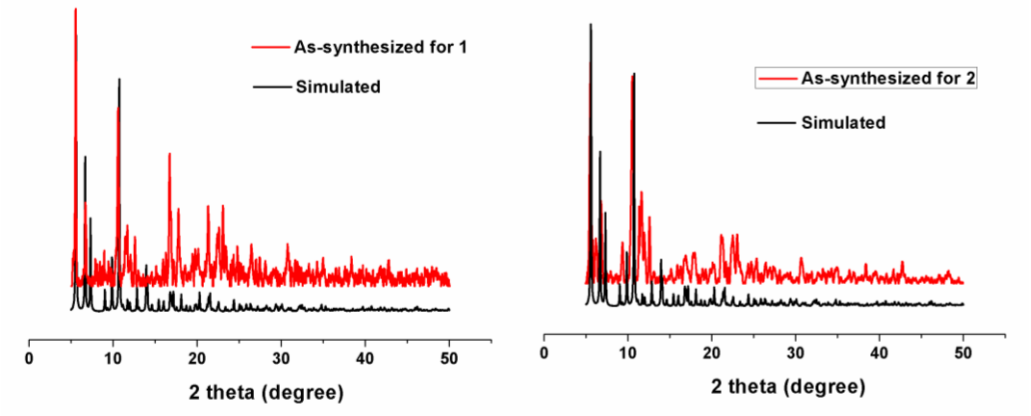

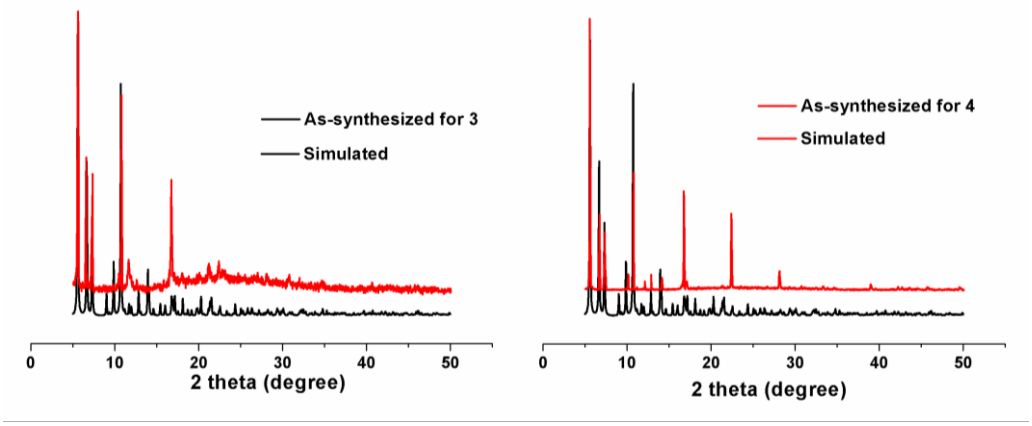

Fig. S1 XRPD patterns for the as-synthesized **1–4** and the simulated patterns from single-crystal X-ray data**.**

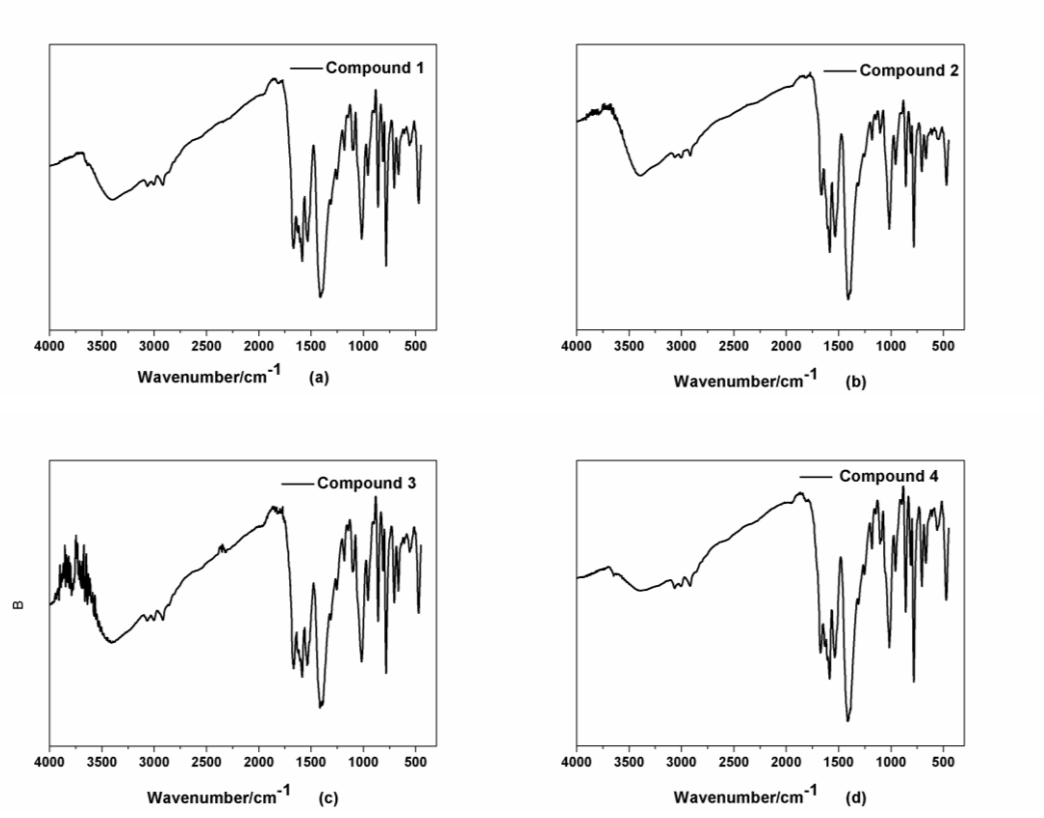

Fig. S2 The IR spectra for compounds **1–4**.

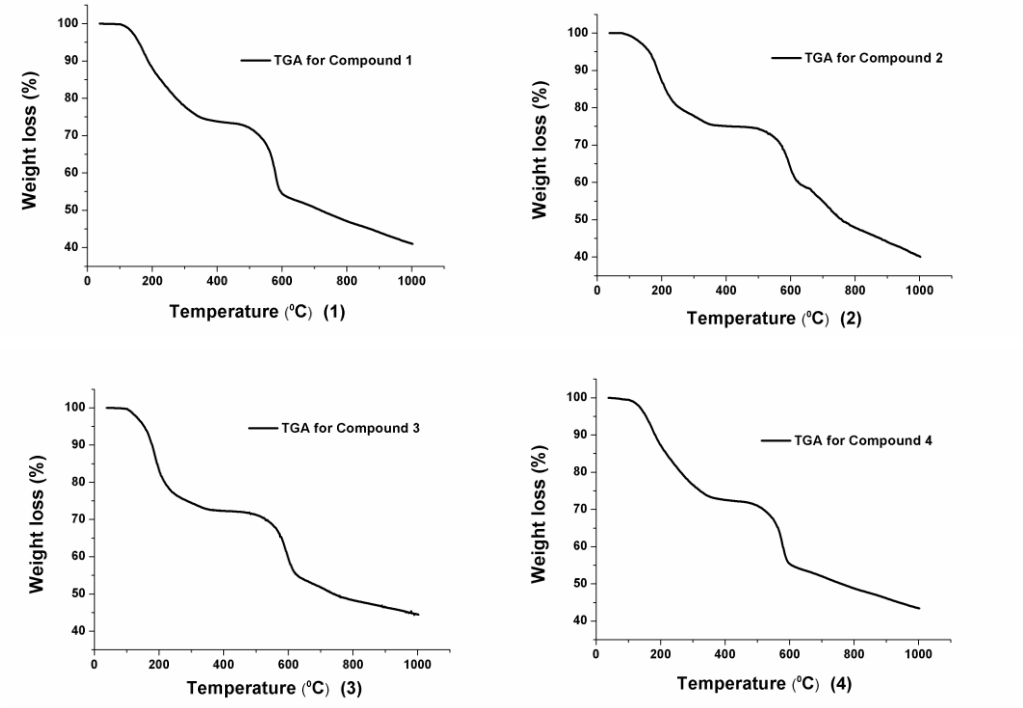

Fig. S3 The TGA curves for **1–4**.

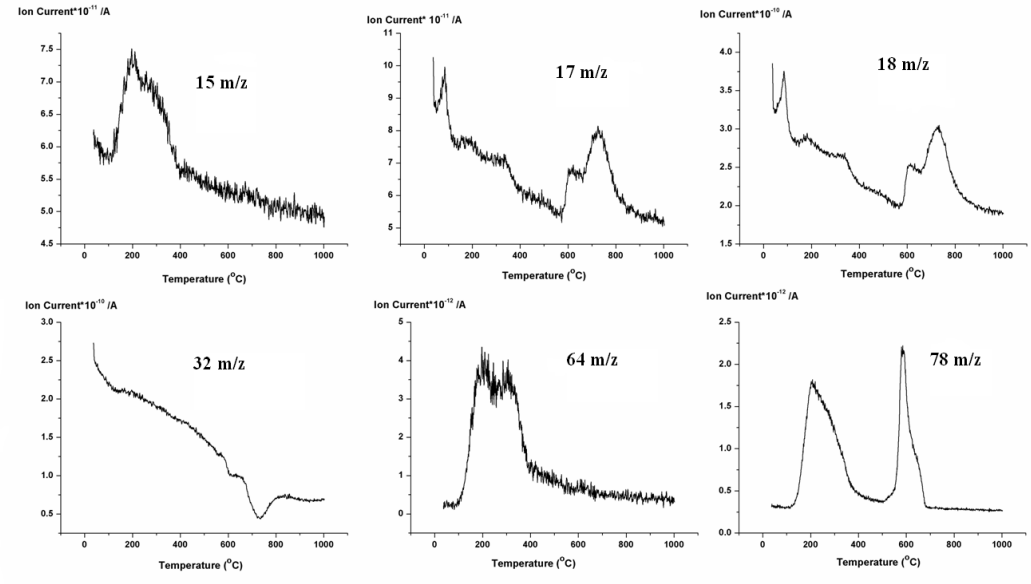

Fig. S4 MS analysis of **1** with different ion current signals.

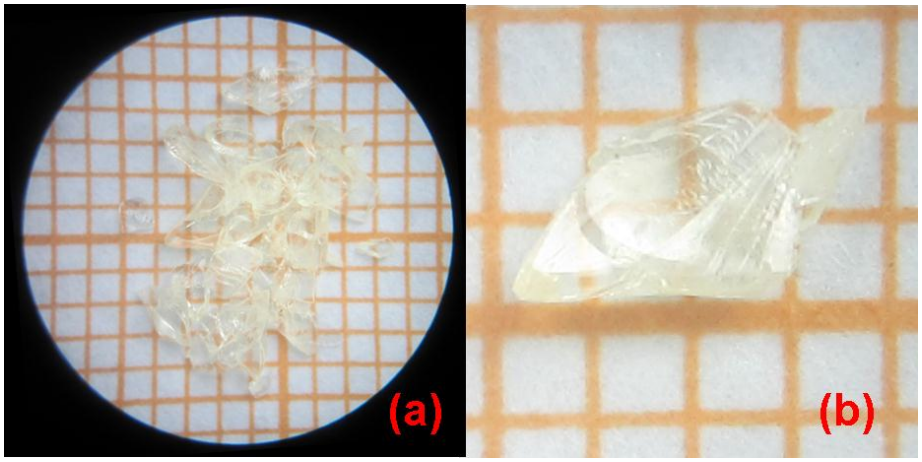

Fig. S5 Photo image of **1**, *ca*. 2.0 × 3.0 × 1.0 mm in dimension.

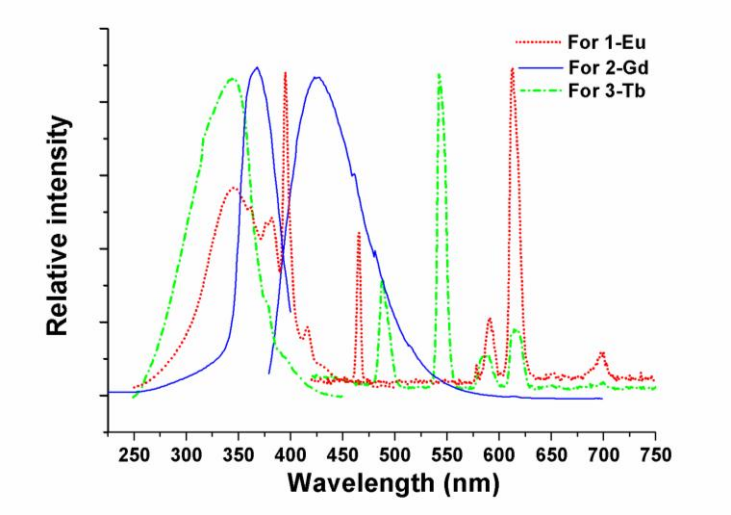

Fig. S6 Solid-state excitation spectra (Left) and emission spectra (Right) for **1**–**3** at room temperature.

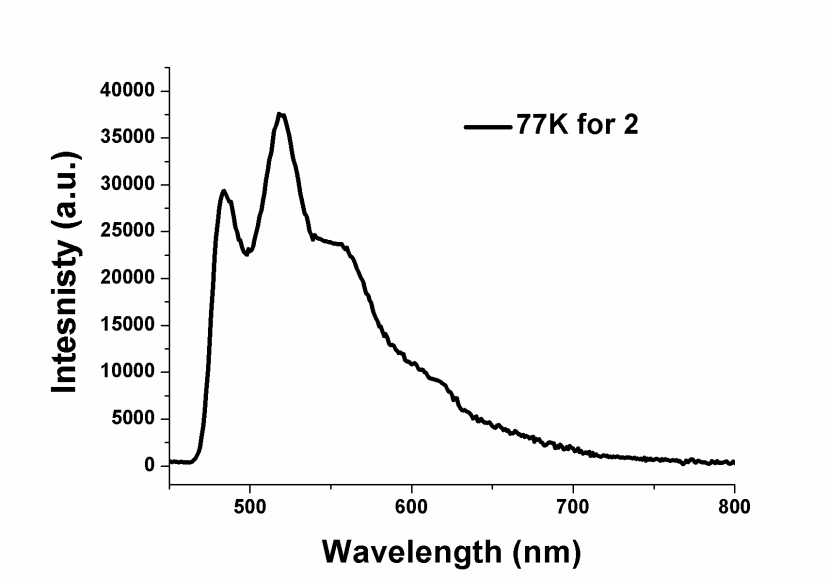

Fig. S7 Solid state emission spectrum of **2** at 77 K.

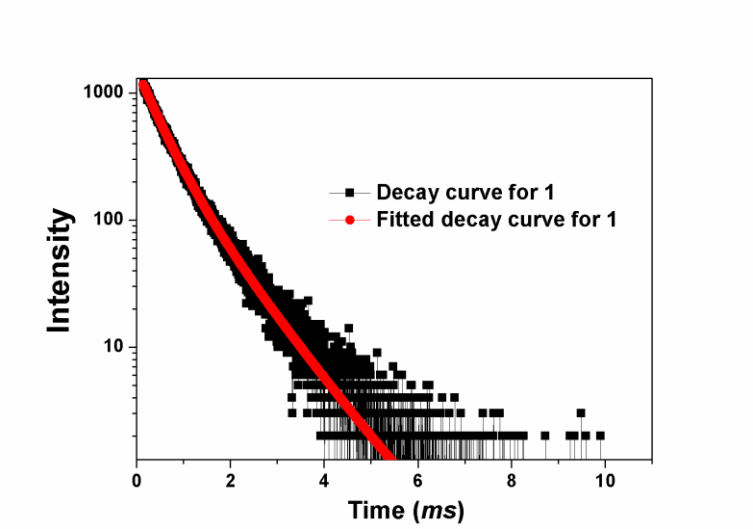

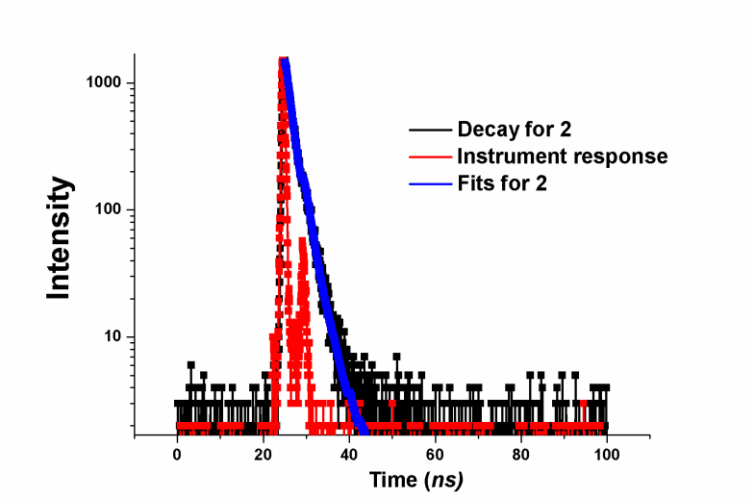

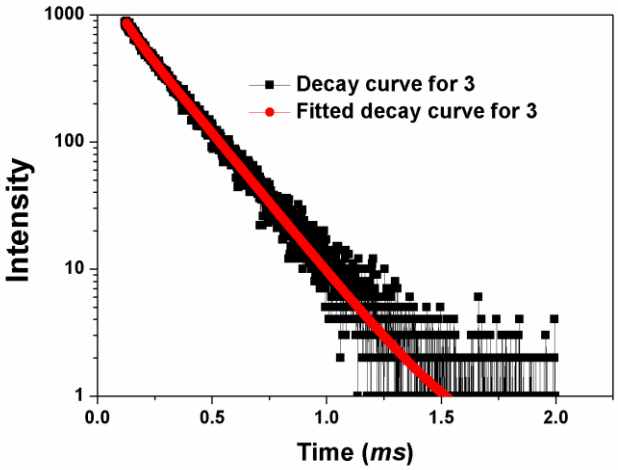

Fig. S8 Decay curves for **1**, **2**, and **3**, determined by monitoring the maximal emissions excited at 345 nm for **1** and **3**, and 365 nm for **2**, respectively.

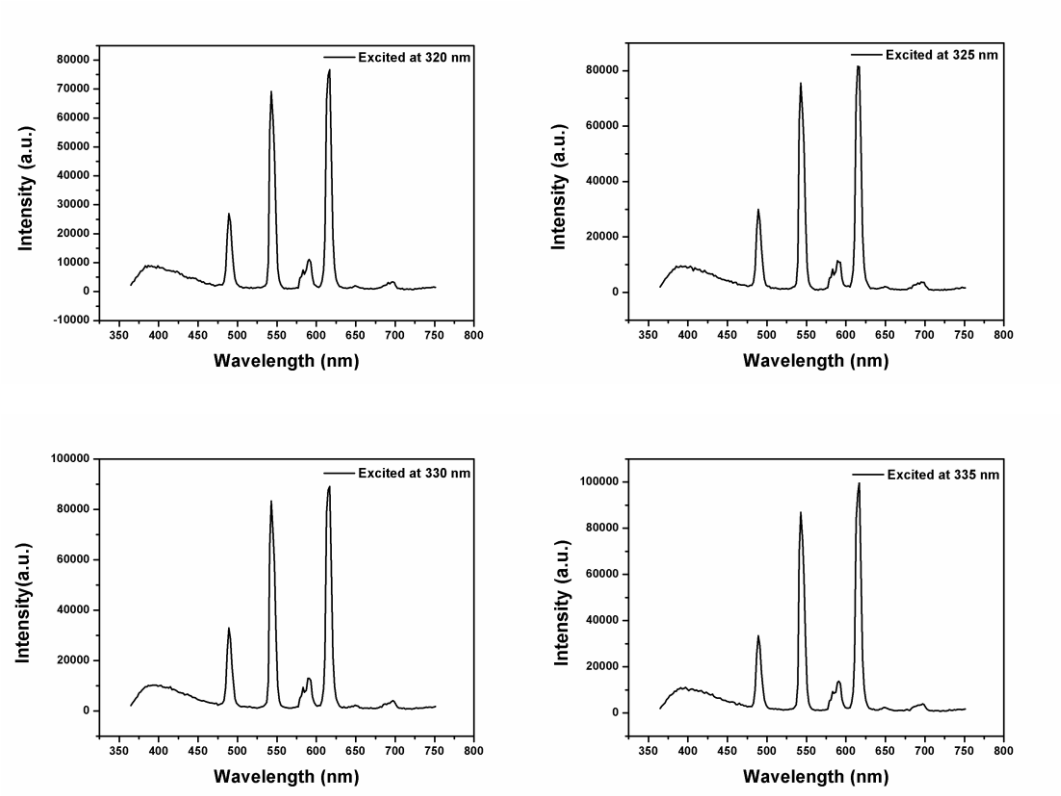

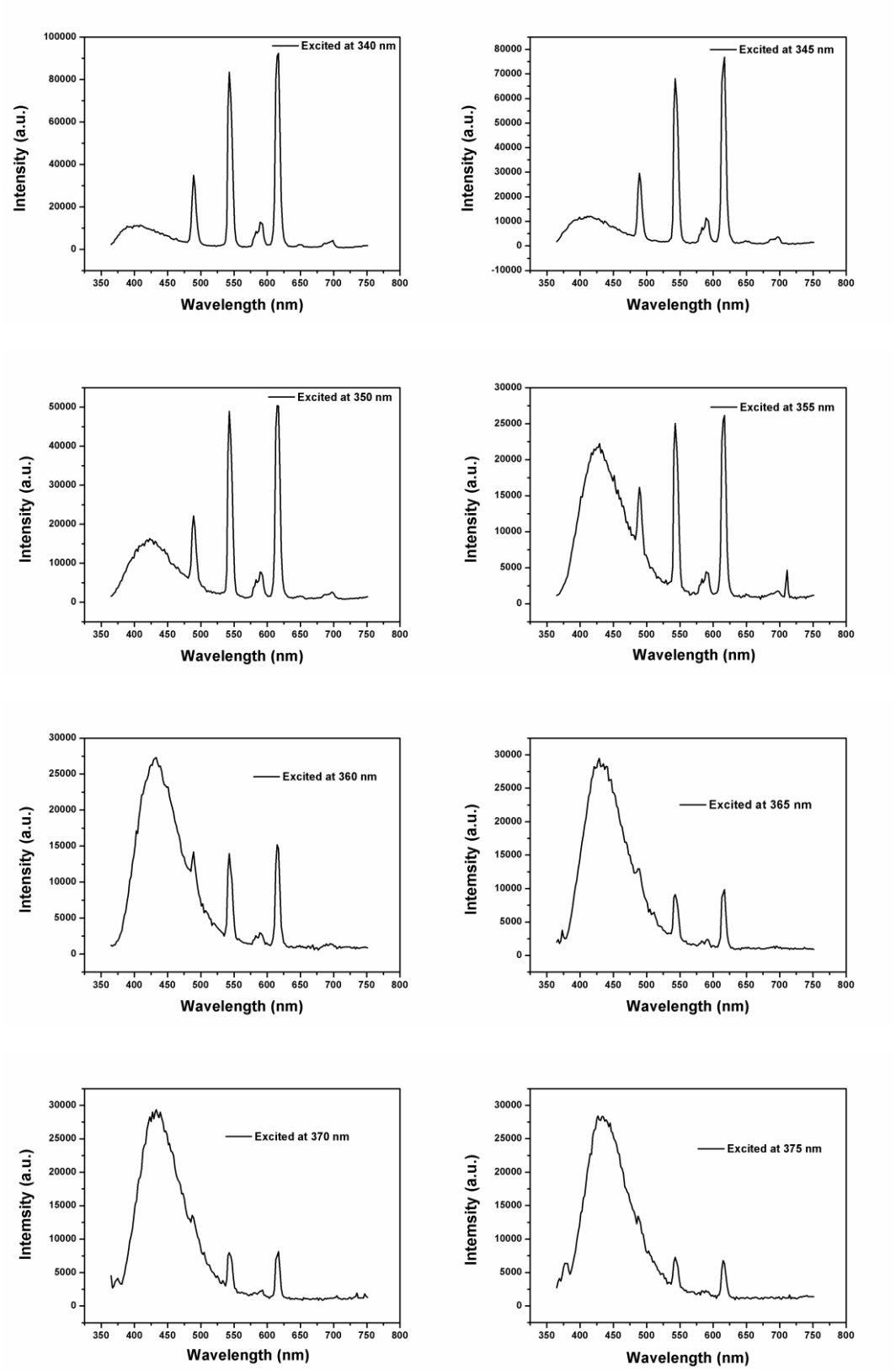

Fig. S9 The co-existence of the Eu^{3+}, Tb^{3+} ions and the ligand based emissions under different excitation.

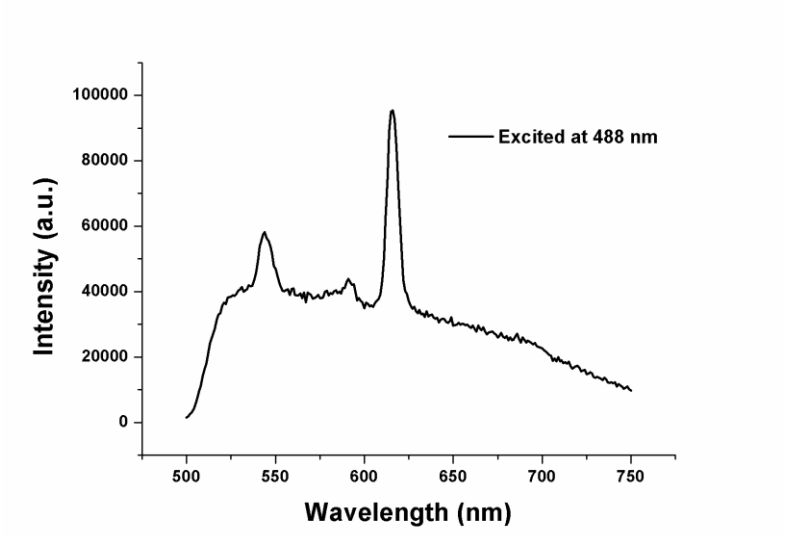

Fig. S10 Room temperature emission spectrum for **4** excited at 488 nm.